Available online at www.sciencedirect.com

ScienceDirect

Ceramics International 40 (2014) 1879–1883

CERAMICS INTERNATIONAL

www.elsevier.com/locate/ceramint

In vivo investigation of biological responses to tricalcium silicate pastes in muscle tissue

Qing Lin[a,*], Wenyan Zhang[a], Chunhua Lu[b], Guihua Hou[c], Zhongzi Xu[b]

[a]School of Material Engineering, Jinling Institute of Technology, Nanjing 211169, China
[b]State Key Laboratory of Materials-Oriented Chemical Engineering, Nanjing University of Technology, Nanjing 210009, China
[c]Key Laboratory for Advanced Technology in Environmental Protection of Jiangsu Province, Yancheng Institute of Technology, Yancheng 224051, China

Received 15 May 2013; received in revised form 16 July 2013; accepted 20 July 2013
Available online 27 July 2013

Abstract

The biocompatibility of tricalcium silicate (Ca_3SiO_5; C_3S) paste was studied by intramuscular implantation. C_3S paste can induce the deposition of apatite layer on its surface in the muscle tissue. The widths of apatite layer between C_3S paste and muscle tissue are increased with the increasing of implantation time. Pure C_3S and fluorine-doped C_3S (F-C_3S) pastes induce less inflammatory reactions to the muscle tissue than PMMA paste. Pure C_3S and F-C_3S pastes are embedded with connective tissue after 12 weeks of implantation as well as PMMA paste. However, more living fibroblasts and fewer macrophages are observed in the connective tissue around F-C_3S paste. F-C_3S paste is better biocompatibility to the muscle tissue than pure C_3S paste, because F-C_3S paste has a better deposition ability of apatite layer. Those results confirm that F-C_3S may be more biologically suitable for bone cement.

Keywords: D. Apatite; Bioactivity; Biocompatibility; Tricalcium silicate; Inflammatory reaction

1. Introduction

Tricalcium silicate (Ca_3SiO_5, C_3S) is intensively investigated as a novel bone cement for dental and orthopedic surgery [1–2], because of its excellent self setting property, bioactivity, degradability and stimulation effect on cell growth in vitro [2–4]. Although C_3S cement would play an important role in hard tissue prosthetics such as bone and teeth, the *in vivo* biocompatibility of C_3S is still under debate. Few studies have reported biocompatibility of C_3S in living tissue, the *in vivo* biocompatibility of C_3S cement should be further evaluated for the clinical applications.

When C_3S paste is used to reconstruct the hard tissue defects, C_3S paste is exposed to not only hard tissues but also various soft tissues (such as bone marrow, fibrous connective tissue and muscle tissue), which generally show more severe responses than hard tissues. Therefore, the objective of this investigation was to evaluate the soft tissue response to C_3S paste. Among many potential bone cements, poly (methyl methacylate) (PMMA) bone cement has been successfully used in orthopedic surgeries, and the biological properties of PMMA are well established [5]. PMMA bone cement is the favorable candidate as control to evaluate the *in vivo* biocompatibility of C_3S cement. For this purpose, C_3S pastes were implanted into the skeletal muscle (rat), and a comparative analysis of biological responses to C_3S pastes was done using PMMA bone cements as control.

2. Materials and methods

2.1. Preparation of materials

Pure C_3S and fluorine-doped C_3S (F-C_3S) powders were prepared according to previously published protocols [6]. Pure C_3S and F-C_3S powders were mixed with deionized water at a liquid to powder (L/P) ratio of 0.5 ml/g, respectively. The homogenous pastes were molded into stainless molds with a diameter of 3 mm and height of 6 mm, and stored at 37 °C and

*Corresponding author. Tel.: +86 18913806402.
E-mail address: lnqing@yahoo.com (Q. Lin).

0272-8842/$ - see front matter © 2013 Elsevier Ltd and Techna Group S.r.l. All rights reserved.
http://dx.doi.org/10.1016/j.ceramint.2013.07.092

100% relative humidity for 24 h. PMMA bone cement was purchased form Tianjing Institute of Synthetic Materials Industry, China. PMMA powder was mixed with PMMA liquid by keeping the L/P ratio at 1.0 ml/g. The homogenous mixture was also molded into stainless molds with the same dimensions as above. Pure C_3S, F-C_3S and PMMA pastes were removed form the molds, and sterilized by UV irradiation for 2 h for implantation.

2.2. Animal experimentation

The animal experimentations were conducted at the Animal Facility in Drum Tower Hospital of Nanjing, affiliated to the Medical School of Nanjing University. The study protocol was submitted to and approved by the local animal care. Experiments were performed using 18 adult white rats weighting 300–400 g. Rats were housed with water and food at will. The animals were placed in quarantine for at least 2 weeks prior to surgery. Rats were under general anesthesia with a halogenous compound. The surgical sites were shaved and disinfected; a lateral skin incision was made along the axis of the femur. An intramuscular pocket was created in the quadriceps muscle using blunt dissection. As-prepared pastes were implanted into the muscle pocket. Muscle and skin were sutured in layers using absorbable sutures. The same procedure was applied bilaterally thus, giving 2 as-prepared pastes per animal. Antibiotic treatment was performed after surgery to reduce the risk of infection. Animals were sacrificed at 1 week, 4 weeks and 12 weeks of implantation using an intra cardiac over dose of sodium pentobarbital. Implants with surrounding full-thickness host tissue were harvested. Samples were retrieved and immediately fixed in neutral formalin for 1 week.

2.3. Characterization of the implants

The fixed sample was dissected carefully to remove visible muscle tissue, and the residual muscle tissue was removed with gauze. Then, the clear sample was transferred into anhydrous ethanol. Finally, the samples were dried in the vacuum oven at 80 °C for 24 h. The powders collected from the surface of dried sample were characterized by Fourier Transform Infrared Spectroscopy (FTIR; Nexus 670, Nicolet, America). The FTIR spectra were collected using the KBr pellet method with a resolution of 2 cm^{-1} and a scan number of 32. The fixed samples were embedded under vacuum in an epoxy resin and gently polished with decreasing grades of diamond powder. The micrographs and element distributions of the interface between implant and muscle were characterized by SEM (JSM-5900, JEOL, Tokyo, Japan) equipped with an energy dispersive X-ray spectrometer (EDX, Thermo Electron, America). SEM micrographs were taken using an acceleration voltage of 5.0 kV. Element distribution images were performed at an accelerating voltage of 15 kV and an electron beam current of 2 nA using a data collection time of 300 s. X-ray photoelectron spectroscopy (XPS; Thermo ESCALAB 250, USA) was carried out by using monochromatised Al Kα X-ray source, and operated at a powder of 150 W. The survey spectra were performed with pass energy of 70.0 eV at a step of 1 eV, and F1s spectra (high resolution scans) were collected with pass energy of 40.0 eV at a step of 0.05 eV.

2.4. Histological analysis

The fixed samples containing pure C_3S and F-C_3S pastes were decalcified in Gooding and Stewart′s fluid. The solution was stirred daily and changed once in 3 days. The decalcified tissues were processed in a routine manner. Because PMMA can not adhere to the surrounding tissues, PMMA was directly removed form the surrounding tissue. The residual tissue was directly embedded in paraffin. The sections were cut and stained with Haematoxylin and Eosin. The histological examination was conducted under light microscopy (Olympus Bx 50). The numbers of cells around the implantation were manually counted and expressed as numbers per mm^2 by image analysis. All the results are expressed as means ± SD. Statistical analyses were accomplished by unpaired Student′s *t*-test.

3. Results and discussion

Surgery was well tolerated in all animals. No erosions or evidences of infection were seen.

3.1. Characterization of the implants

C_3S powder has an important property to set in humid and wet environments, such as water, blood and other fluids [7]. C_3S paste mainly consists of crystalline $Ca(OH)_2$ and amorphous calcium silicate hydrate (C–S–H) gel, and there is a wide consensus that hydrated C_3S paste could induce the deposition of apatite in simulated body fluid (SBF) with the ion concentrations nearly to those of human blood plasma [2,6]. FTIR spectra of pure C_3S and F-C_3S paste surface implanted in muscle tissue for 1 week are shown in Fig. 1. The partially resolved doublet peaks at 1430 and 1480 cm^{-1} are attributed to carbonate species for the carbonation reaction of $Ca(OH)_2$ by incorporated with HCO_3^- in body plasma [8]. The broad bands at 1646 and 3451 cm^{-1} arise from O-H vibrations of free water in the pore of C_3S paste. The stretching mode of O–H in $Ca(OH)_2$ gives rise to a signal at 3643 cm^{-1} [9]. The characteristic peak at 977 cm^{-1} indicates the polymerization and formation of C–S–H gel in C_3S paste [10]. As our previous research [6], new peaks at ~600 and 1040 cm^{-1} are assigned to P–O bending vibration and stretching vibrations, respectively. The broad peak at 600 cm^{-1} is an indicator of the deposition of amorphous apatite on pure C_3S and F-C_3S paste surfaces [7]. It is confirmed that C_3S paste could induce the apatite formation on its surface in muscle tissue.

SEM micrographs and element (Ca, Si and P) distributions of the interfaces between muscle tissue (rat) and pure C_3S paste are shown in Fig. 2. It indicates that an apatite layer containing Ca and P element deposits around pure C_3S paste. The width of apatite layer is 20 μm at 1 week, 40 μm at 4 weeks and 140 μm at 12 weeks. It also indicates that the width of apatite layer increased with the increased implantation time. F-C_3S paste could also induce the apatite layers with the similar widths to those induced

by pure C_3S paste. The apatite layers induced by F-C_3S paste have the same characterization as that induced by pure C_3S paste. Those results gave good supports that C_3S paste is bioactive.

The XPS had been employed to further understand the formation of apatite, and the result is shown in Fig. 3. The P_{2p} peak had been detected in the interface after F-C_3S paste implanted for 1 week (Fig. 3a), this result agrees with the FTIR results (Fig. 1). The XPS survey spectrum of pure C_3S paste is same as that of F-C_3S paste (Fig. 3a). However, the appearance of F_{1s} peak at 683.8 eV indicates the formation of F-substituted apatite in the interface after F-C_3S paste implanted for 1 week (Fig. 3b) [11]. These were attributed to the lowest Ksp (6.5×10^{-65} for $x=0.56$) of F-substituted apatite ($Ca_5(PO4)_3OH_{1-x}F_x$) as compared with hydroxyapatite ($Ca_5(PO4)_3OH$, $K_{sp}=7.36 \times 10^{-60}$) [12,13]. Combined with our previous study [6], it indicates that F-C_3S paste could induce the formation of F-substituted apatite in a shorter time than pure C_3S paste.

3.2. Histological observation

The histological micrographs of muscle tissues around PMMA paste, pure C_3S paste and F-C_3S paste are shown in

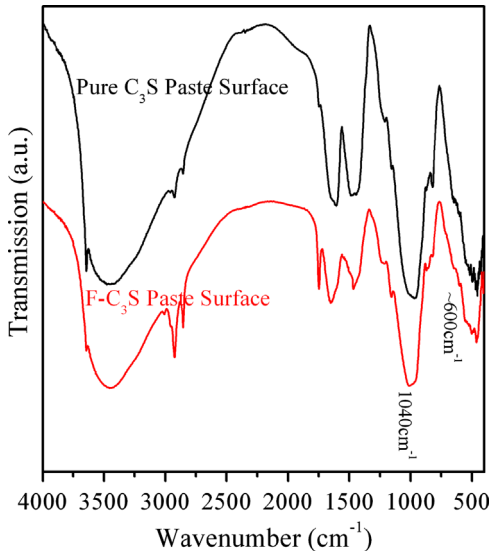

Fig. 1. FTIR spectra of pure C_3S and F-C_3S paste surfaces implanted in muscle tissue (rat) for 1 week.

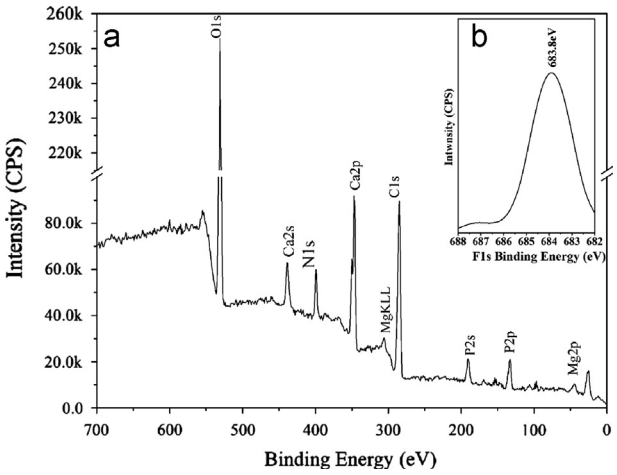

Fig. 3. XPS survey spectrum (a) and XPS F_{1s} spectrum (b) of the interface between F-C_3S paste and muscle tissue after implanted for 1 week.

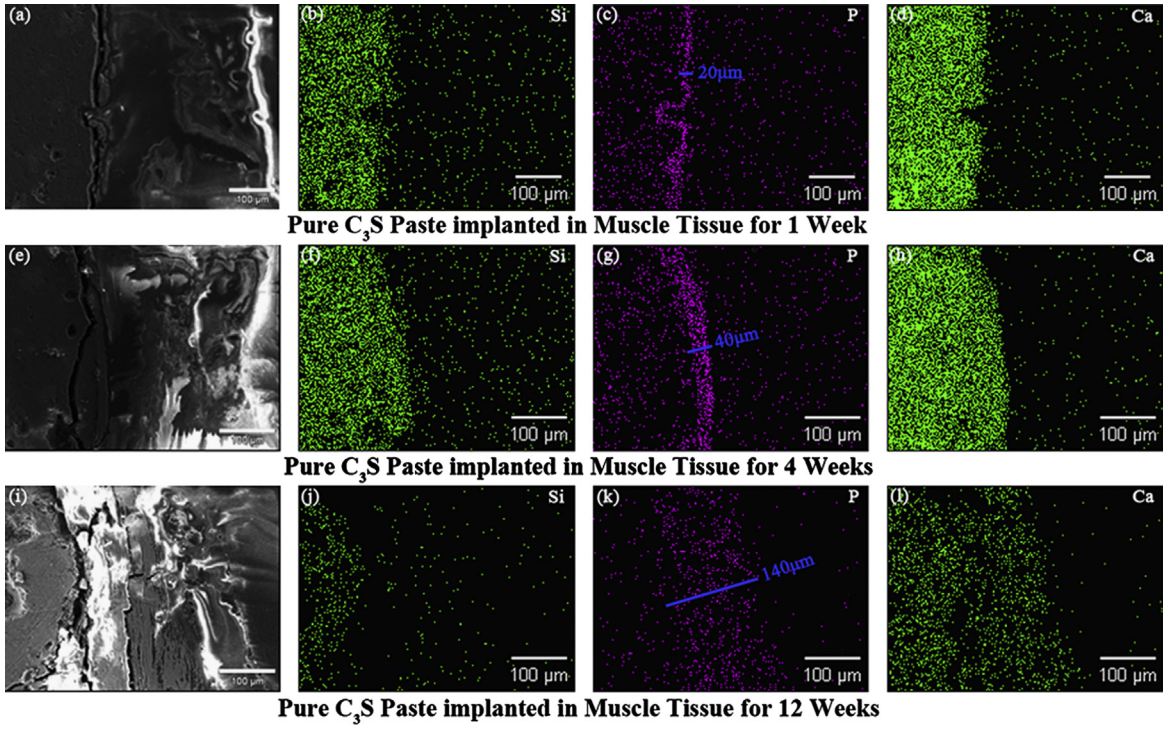

Fig. 2. SEM micrographs and element (Si, P and Ca) distributions of the interfaces between muscle tissue (rat) and pure C_3S paste.

Fig. 4. In agreement with previous studies [14], an extensive inflammatory is observed around PMMA paste (Fig. 4a). The inflammatory zone contains numerous fibroblasts, macrophages and foreign body giant cells without any muscle necrosis (Fig. 4a). Those cells are extending into adjacent muscle tissue. The numbers of those cells in the surrounding tissue of PMMA, pure C_3S and F-C_3S pastes were counted by image analysis as well (Fig. 5). Giant cells are generated in response to the presence of a large foreign body. This is particularly evident with implants that cause the tissue chronic inflammation and foreign body response. The width of the above-described inflammatory zone was ~200 μm at 1 week, ~100 μm at 4 weeks. The appearance of giant cells as evidence of acute inflammation (Fig. 4 and Fig. 5) may be attributed to the local effects of methyl mthacrylate (MMA) monomer leaching out of PMMA paste [14]. After implanted for 12 weeks, PMMA paste is embedded with a mature connective tissue (fibrous encapsulation) with few inflammatory cells and fibroblasts (Fig. 4c and Fig. 5a).

After 1 week and 4 weeks of implantation, a mild inflammatory response to pure C_3S paste was observed with the appearances of fibroblasts and macrophage, with no signs of foreign body giant cells (Figs. 4 and 5). At 12 weeks (Fig. 4f), the connective tissue around pure C_3S paste was characterized by inner layer comprised with few fibroblasts and outer layer populated with some macrophages (Fig. 5).

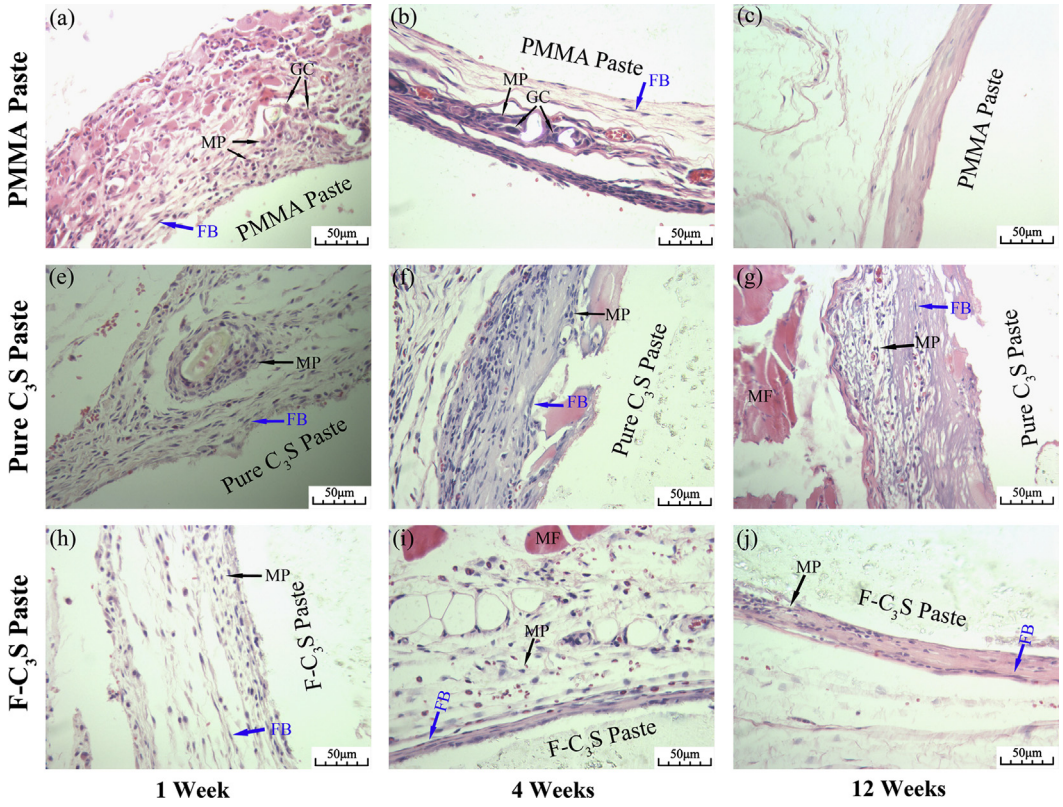

Fig. 4. Histological micrographs of muscle tissues (rat) around PMMA paste (a, b, c), pure C_3S paste (d, e, f) and F-C_3S paste (h, i, j). MF: muscle fiber; FB: fibroblast; MP: macrophage; GC: foreign body giant cells.

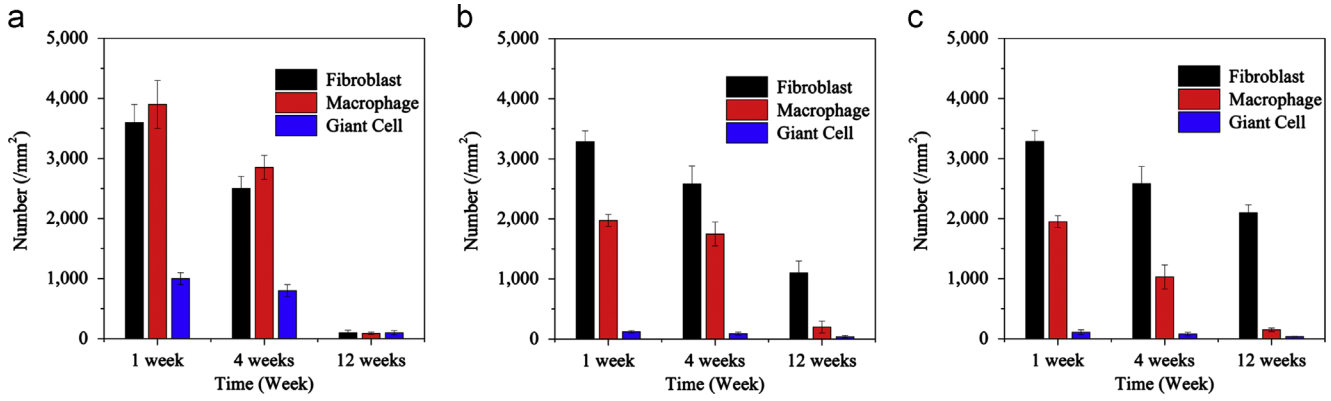

Fig. 5. Numbers of cells counted in the surrounding tissue of PMMA(a), pure C_3S(b) and F-C_3S(c) paste.

It indicates that the connective tissue around pure C_3S paste becomes mature.

As comparing with PMMA and pure C_3S paste, F-C_3S paste provokes a less inflammatory response to muscle tissue around F-C_3S paste at 1 week and 4 weeks, because fewer macrophages could be observed in the inflammatory zone (Figs. 4 and 5). However, the connective tissue around F-C_3S paste mainly contains more living fibroblasts at 12 weeks (Fig. 5c). Moreover, the width of connective tissue around F-C_3S paste is significantly thinner than that around pure C_3S paste (Figs. 4f and j).

It is well known that foreign body reaction in living body consists of a series of biological reactions. Namely, inflammatory cells infiltrate around the foreign body in the early phase. Then, the foreign body is surrounded by granulation tissue and/or fibrous capsule in the late phase. The histological reactions around PMMA, pure C_3S and F-C_3S pastes are essentially similar to the above described foreign body reaction. However, the histological response to material also depends on the bioactivity of materials. PMMA is well known as an inert material [5], it is easy understood that bioactive pure C_3S pastes and F-C_3S paste show better biocompatibility to muscle tissue than PMMA. Moreover, our previous study had proved that F-C_3S paste could induce the formation of F-substituted apatite in a shorter time than pure C_3S paste [6]. The earlier formation F-substituted apatite layer on F-C_3S paste surface may promote cell adhesion, and endow its less inflammation reaction in muscle tissue. The thin connective layer observed between the muscle and F-C_3S paste revealed how well accepted this material is in the biological environment. These reassuring results promote us to continue our study on F-C_3S in the future, performing bone implants and comparing the results with those well-known materials. Therefore, F-C_3S is considered to be the potential bone cement. However, further evaluation from various viewpoints should be performed in the near future.

4. Conclusions

The biocompatibility of C_3S paste was studied by intramuscular implantation in rats. It indicates that C_3S paste can induce the deposition of apatite layer on its surface in muscle tissue. The widths of apatite between C_3S paste and muscle tissue are increased with the increasing of implantation time. Pure C_3S and F-C_3S paste induce less inflammatory reactions to muscle than PMMA paste. Although the connective tissue is formed between C_3S paste and muscle tissue, F-C_3S paste shows a better biocompatibility to muscle than pure C_3S paste, because F-C_3S paste has a better deposition ability of apatite layer. F-C_3S may be more biological acceptability as bone cement.

Acknowledgments

This research was supported by National Natural Science Foundation of China (51103066), Educational Commission of Jiangsu Province (12KJD150006), Research Program of Jinling Institute of Technology (JIT-B-201233) and Key Laboratory for Advanced Technology in Environmental Protection of Jiangsu Province (AE201308).

References

[1] Q. Lin, X. Lan, Y. Li, C. Lu, Z. Xu, Anti-washout carboxymethyl chitosan modified tricalcium silicate bone cement: preparation, mechanical properties and in vitro bioactivity, Journal of Materials Science: Materials in Medicine 21 (12) (2010) 3065–3076.

[2] W. Zhao, J. Wang, W. Zhai, J. Chang, The self-setting properties and in vitro bioactivity of tricalcium silicate, Biomaterials 26 (31) (2005) 6113–6121.

[3] P. Laurent, J. Camps, M. De Meo, J. Dejou, I. About, Induction of specific cell responses to a Ca_3SiO_5-based posterior restorative material, Dental Materials 24 (11) (2008) 1486–1494.

[4] W. Peng, W. Liu, W. Zhai, L. Jiang, L. Li, J. Chang, Effect of tricalcium silicate on the proliferation and odontogenic differentiation of human dental pulp cells, Journal of Endodontics 37 (9) (2011) 1240–1246.

[5] G. Lewis, Properties of acrylic bone cement: state of the art review, Journal of Biomedical Materials Research 38 (3) (1997) 155–182.

[6] Q. Lin, Y. Li, X. Lan, C. Lu, Z. Xu, The apatite formation ability of CaF_2 doping tricalcium silicates in simulated body fluid, Biomedical Materials 4 (4) (2009) 045005.

[7] Q. Lin, X. Lan, Y. Li, C. Lu, Z. Xu, Preparation and in vitro bioactivity of zinc incorporating tricalium silicate, Materials Science and Engineering: C 31 (3) (2010) 629–636.

[8] Q. Lin, X. Lan, Y. Li, C. Lu, Z. Xu, Preparation and characterization of novel alkali activated nano silica cements for biomedical application, Journal of Biomedical Materials Research 95B (2) (2010) 347–356.

[9] N.J. Coleman, K. Awosanya, J.W. Nicholson, Aspects of the in vitro bioactivity of hydraulic calcium (alumino) silicate cement, Journal of Biomedical Materials Research 90 A (1) (2009) 166–174.

[10] M.Y.A. Mollah, W. Yu, R. Schennach, D.L. Cocke, A Fourier transform infrared spectroscopic investigation of the early hydration of Portland cement and the influence of sodium lignosulfonate, Cement and Concrete Research 30 (2) (2000) 267–273.

[11] K. Cheng, S. Zhang, W. Weng, The F content in sol-gel derived FHA coatings: an XPS study, Surface and Coatings Technology 198 (1) (2005) 237–241.

[12] E.C. Moreno, M. Kresak, R.T. Zahradnik, Fluoridated hydroxyapatite solubility and caries formation, Nature 247 (1974) 64–65.

[13] M. Iijima, J. Moradian-Oldak, Control of apatite crystal growth in a fluoride containing amelogenin-rich matrix, Biomaterials 26 (13) (2005) 1595–1603.

[14] P.A. Revell, M. Braden, M.A.R. Freeman, Review of the biological response to a novel bone cement containing poly(ethyl methacrylate) and n-butyl methacrylate, Biomaterials 19 (17) (1998) 1579–1586.